

Inherent Flexibility of Calmodulin Domains: A Normal-Mode Analysis Study

N. P. Barton, C. S. Verma,* and L. S. D. Caves*

Structural Biology Laboratory, Department of Chemistry, University of York, York YO10 5DD, U.K.

Received: August 6, 2002

The distinct character of the two calmodulin (CaM) domains is reflected in different calcium and target interaction affinities, with the C-terminal domain generally showing the higher affinities. We address the distinct properties and roles of the CaM domains by using computer simulations to examine the relative flexibility of the two domains. We used extensive molecular dynamics simulations of the individual domains to sample their conformational space. From this sample of conformations, we performed multiple normal-mode analyses to compute vibrational and thermodynamic properties. We see higher intrinsic flexibility of the C-domain compared with that of the N-domain. Furthermore, in a simulation of a CaM-target peptide complex, the C-domain conformation maintains its conformation better and has lower atomic RMS fluctuations than the N-domain. These results tie in with the observed differentiation of roles of the CaM domains.

Introduction

Calmodulin (CaM) is an intracellular second messenger calcium-signaling molecule that is ubiquitous in eukaryotic systems. The free Ca^{2+} concentration in the extracellular matrix is generally close to 10^{-3} M whereas the intracellular concentration is normally less than 10^{-7} M. Transient opening of the Ca^{2+} channels in the cellular membrane allows this level to increase to 10^{-6} M, which is sufficient to activate CaM by enabling a conformational change. This results in the activation of numerous different cellular processes¹ through the participation of several proteins including, among others, autoinhibitory regions of various protein kinases, phosphodiesterases, and nitric oxide synthases. The key to CaM function is the ability of the protein to accommodate a wide range of different target fragments of diverse primary sequences, the only common feature of which is a high propensity for helix formation.²

The crystal structure of Ca^{2+} -CaM indicates two Ca^{2+} -binding domains each containing two EF-hand motifs that are connected by a long helical flexible tether³ (Figure 1a and b). The flexibility of this tether allows the two Ca^{2+} -binding domains to come together and to encompass CaM-binding domains in other systems (Figure 1c). Examples of various CaM target complexes have been determined by both X-ray crystallography⁴ and NMR.⁵ Although a large degree of cooperativity in Ca^{2+} binding is observed *within* each domain, the differences in Ca^{2+} affinities *between* the two domains result in largely independent activation of targets at different Ca^{2+} concentrations.⁶ Despite the high sequence homology observed for the two domains of CaM, it seems clear that rather than being ambidextrous the N and C domains of CaM have different characteristics and thus different roles.

CaM is a highly flexible system. NMR studies have indicated that Ca^{2+} -free CaM exhibits considerably more conformational sampling than the Ca^{2+} -bound form of the protein⁷ and that the backbone flexibility of the system is further reduced by the presence of a target peptide. Experimental structure determination of CaM is complicated by the dynamic properties of the

system, which contribute to conformational averaging (in the case of NMR) and nonresolvable regions (in the crystallographic electron density). This is particularly apparent at the N terminus of the protein and in the central linker. Such flexibility is characteristic of signaling proteins that generally participate in low-affinity, low specificity interactions, in contrast to catalytic systems, which are more conserved and better ordered in crystal structures.⁸ Even in an atomic resolution ($d_{\text{min}}=1.0$ Å) low-temperature crystal structure of CaM,⁹ significant disorder was observed throughout the protein, and the anisotropic B factors revealed scissor-type opening/closing motions within each of the EF hands. More recently, however, NMR experiments incorporating restraints from residual dipolar couplings (RDC) have suggested a structure for the CaM domains¹⁰ with a conformation that lies between the Ca^{2+} -bound (observed crystallographically) and Ca^{2+} -free structures (observed by NMR, Figure 3b). Computational molecular dynamics simulations have also been applied to investigate the dynamics and flexibility of CaM.^{11–13} A comparison of the experimentally determined structures and simulated trajectories suggests greater conformational flexibility for the N domain of the protein compared to that of the C domain. This result is of interest in the context of experimental observations that the C domain of CaM has a greater affinity for Ca^{2+} and some CaM targets whereas the N domain is less specific in its choice of target motif.¹⁴

We present results of computer simulations that probe the structure and dynamics of the individual CaM domains. Molecular dynamics (MD) is used to sample the conformational space of the protein, and the conformational flexibility of the two domains is then investigated using classical normal-mode analysis (NMA).

Methods

Computations were carried out for the separate lobes of CaM using the 1.0-Å crystal structure (RCSB entry 1exr⁹). Fragments corresponding to the regions E2-A73 and L85-S147 were used for the N and C-term lobes, respectively. For residues with multiple conformations, the first listed (or “A”) conformer was used. Additionally, computations on the CaM–CaMKIIa com-

* Corresponding authors. E-mail: chandra@ysbl.york.ac.uk; caves@ysbl.york.ac.uk.

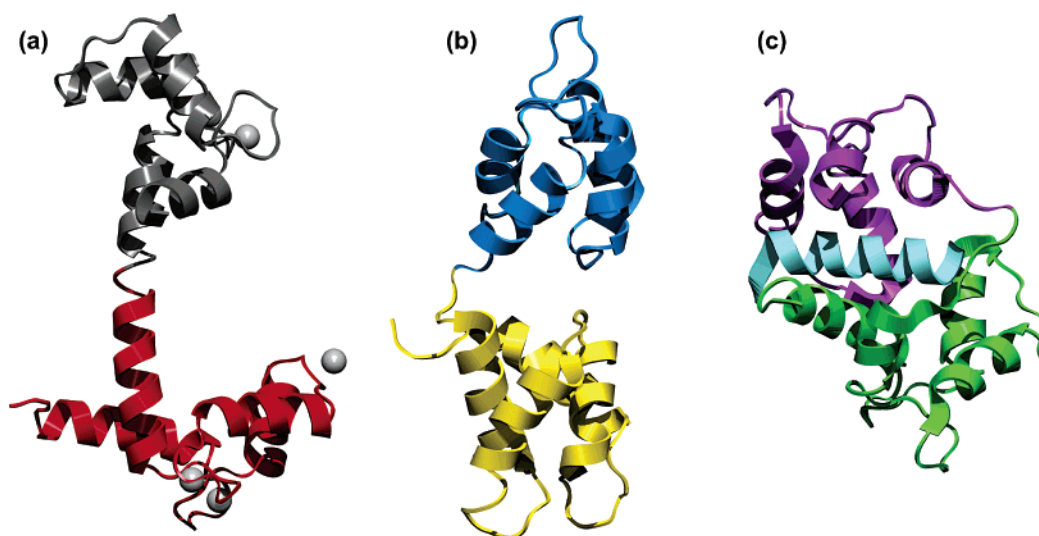


Figure 1. Ribbon protein cartoon representations of calmodulin in the (a) Ca^{2+} -loaded conformation (RCSB entry 1exr⁹), (b) Ca^{2+} -free conformation (RCSB entry 1dmo, model 28³⁰), and (c) in complex with the CaM binding domain of CaM kinase II (RCSB entry 1cm4¹⁵). The N- and C-term Ca^{2+} -binding domains are highlighted in different colors corresponding to the color coding of the related trajectories in other figures.

TABLE 1: Summary of MD Simulations Performed

code	description	no. of atoms
ntsolv	N-term lobe Ca^{2+} -bound 10-ns simulation	4694
ntapo	N-term lobe Ca^{2+} -expulsion 10-ns simulation	4691
ctsolv	C-term lobe Ca^{2+} -bound 10-ns simulation	4214
ctapo	C-term lobe Ca^{2+} -expulsion 10-ns simulation	4212
complex (ntcomp and ctcomp)	Ca^{2+} -CaM-CaMKIIa complex structure 10-ns simulation	9188

plex were carried out on the first model (chains A and B) of a 2.0-Å crystal structure (RCSB entry 1cm4¹⁵). The structure resolved in the experiment included residues L4-T146 of CaM and the peptide corresponding to a fragment of the CaM binding domain of CaMKIIa (residues F293-T310). Table 1 lists the number of atoms included in each simulation.

The CHARMM param19 force field^{16,17} was used to represent the system with all heavy atoms and only the polar hydrogen atoms included explicitly. The solvent was treated using the TIP3 water model.¹⁸ The N and C termini of both protein and peptide fragments were patched with acetyl groups to terminate the truncated sequence. Missing coordinates were built using standard geometrical parameters whereas hydrogen atoms were added using iterations of the HBUILD functionality¹⁹ of CHARMM. The systems were solvated using the Solvate program (kindly provided by Professor H. Grubmüller²⁰) with a shell of water molecules to a minimum thickness of 5.0 Å. A fixed dielectric with a constant ($\epsilon_r = 1.0$) was used. Electrostatic forces were shifted to zero at 12.0 Å, and the van der Waals potential was treated with a switching function acting between 8.0 and 12.0 Å. The nonbonded cutoff was sufficiently large to incorporate interactions between the adjacent Ca^{2+} sites in the CaM fragments, which are less than 12 Å in the crystal structure.²¹

The solvated protein fragments were initially minimized using the steepest descent and adopted basis Newton–Raphson methods. The structures were then heated for 10 ps at 25 K increments to 300 K by coupling the system to a heat bath using a coupling time constant of 0.01 ps.²² At this point, the temperature coupling was loosened to 0.5 ps, the trajectories

were continued to 10 ns, and the coordinates were saved every picosecond. Ca^{2+} -free simulations were generated by the removal of the Ca^{2+} ions from the system immediately after the MD heating phase. Prior to analysis, the saved coordinates were reoriented relative to the initial minimized structure by least-squares superposition²³ to remove any global rotations/translations. Structures were then selected such that the RMS difference between consecutive selected structures was at least 0.13 Å. The threshold was adapted in a manner analogous to that of Elber and Karplus²⁴ for each simulation to select approximately 100 structures from the 10-ns trajectory to represent the entire conformational space explored. The details of the simulations with trajectory names are summarized in Table 1. An eigen analysis of the covariance matrix of the conformers selected for the NMA studies was performed to obtain the principal components of the distribution of conformers generated for the N and C domains separately using the R statistical package.²⁵

At this point, explicit solvent atoms were removed from the selected structures, and they were subjected to extensive energy minimization (convergence criterion was the norm of the gradient vector less than 1×10^{-8} kcal mol⁻¹ Å⁻¹) with a distance-dependent ($\epsilon_r = r_{ij}$ in Å) dielectric constant. The VIBRAN module²⁶ of CHARMM was used to diagonalize the full Hessian, and the normal modes of vibration were computed. The thermodynamic properties (within the classical harmonic oscillator formalism) were evaluated over all the ($3N - 6$) non-rotational–translation modes. In the case of the simulation of the CaM target complex, modes were calculated for the fragments corresponding to the N and C domains while the rest of the system was kept fixed using the reduced basis functionality of CHARMM.²⁷

Results and Discussion

The RMS atomic fluctuations of the systems (Ca atoms) over the simulations are 0.73 (ntsolv), 0.51 (ntapo), 0.52 (ntcomp), 0.44 (ctsolv), 0.61 (ctapo), and 0.24 Å (ctcomp), respectively. Plots of the RMSD versus the initial structure for the selected conformations for each of the simulations (Figure 2) indicate a variety of conformational changes over the course of the MD trajectories. Ntsolv clearly demonstrates a significant conformational change 4 ns into the simulation. This behavior is also

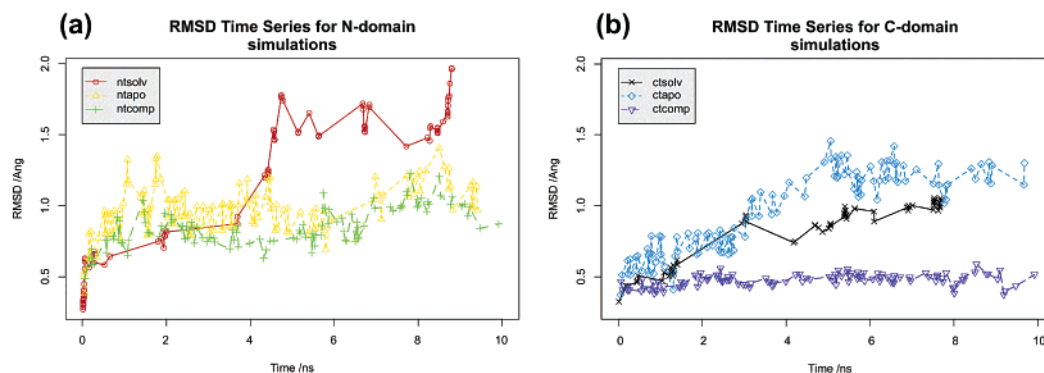


Figure 2. RMSD time series for the five different trajectories. Differences are referenced to (a) the N domain and (b) the C domain of the crystal structure 1exr used for the simulation of free CaM after the least-squares superposition of the fragments. These values are for the C α atoms of the conformations obtained from the MD trajectories prior to minimization for the NMA analysis.

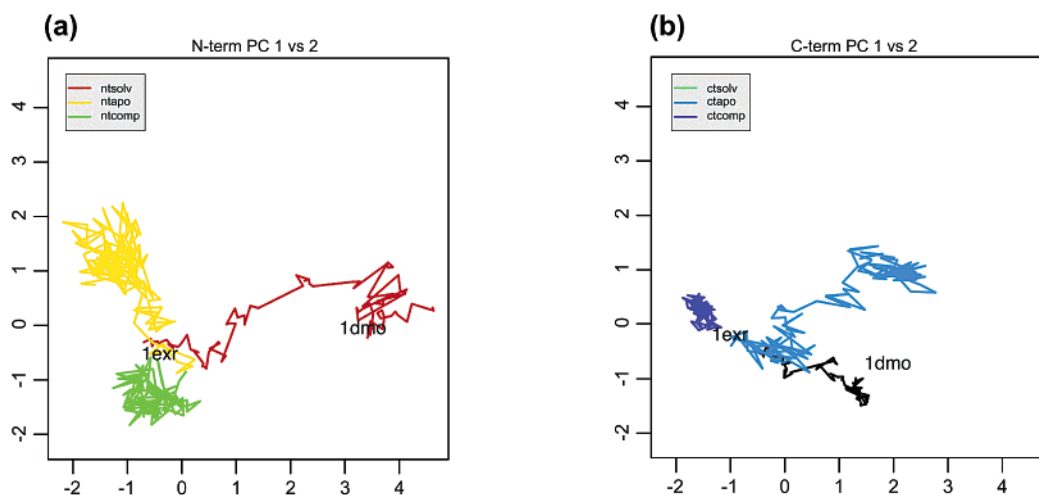


Figure 3. Conformational subspace projections for the first two principal components of the distribution of conformations generated from the MD simulations of the (a) N and (b) C domains of CaM. PCs 1 and 2 together describe 64% of the observed distribution for the N term and 67% of the C term. The MD trajectories are illustrated by solid lines corresponding to the colors indicated in the legend. Projections of conformations corresponding to the experimentally determined structures for Ca $^{2+}$ -bound CaM (1exr) and Ca $^{2+}$ -free CaM (1dmo) onto the subspace are indicated by the corresponding PDB codes. The axes are scaled to indicate conformational differences related to the conventional RMSD in angstroms.

seen in the simulations of Vigil et al.,¹² which also demonstrate a conformational change from the classical Ca $^{2+}$ -bound conformation to that of the Ca $^{2+}$ -free conformation. Principal component analysis (PCA) of the resulting trajectories (Figure 3)^{28,29} demonstrated that the trajectory explored various different conformational subspaces with an initial conformation similar to that of the starting structure 1exr⁹ (Figure 1a) and a final conformation that showed a greater similarity to the experimentally determined structure for Ca $^{2+}$ -free CaM (RCSB entry 1dmo;³⁰ Figure 1b). Interestingly, even though the ntapo trajectory samples several conformational substates, the sampling is not as extensive as for ntsoiv. More surprisingly, it does not explore a conformation similar to the experimentally observed Ca $^{2+}$ -free structure even at 10-ns time scales.

In comparison to the N-term simulations, the C-term fragments of the protein show somewhat reduced overall flexibility. The simulation of the Ca $^{2+}$ -free fragment, ctapo, shows greater conformational flexibility over the 10-ns period than the Ca $^{2+}$ -bound ctsoiv simulation. This is in accord with suggestions from the NMR solution structures of the protein.⁷ The first 5 ns of the ctapo trajectory exhibits significant conformational changes as the effects of the Ca $^{2+}$ removal propagate through the system, resulting in an apparently stable conformation that is conserved for the second half of the trajectory.

The simulation of the CaM target complex exhibits marked differences between the behavior of the N and C domains of

the protein. The N domain of the protein explores a variety of different conformations over the 10-ns simulation, ranging within RMSDs of 0.5 to 1.3 Å to the crystal structure 1exr. The conformation of the C-term lobe in the simulation of the complex, however, is highly conserved throughout the 10 ns of simulation, remaining close to that found for the domain in the absence of a target peptide.

These simulations indicate marked differences in the behavior of the two Ca $^{2+}$ -binding domains of CaM in solution dynamics experiments. Ours and other studies have shown, however, that MD simulations of proteins can be very sensitive to initial conditions (of conformation and momentum) reflecting the high-dimensional and multimimum nature of the potential energy surface.^{13,29} This character may only be amplified in the case of signal transduction proteins, whose architecture is primed for conformational switching.⁸ Only by comparison of tens of simulated trajectories on this time scale could realistic conclusions be drawn regarding the full extent of the conformational space accessible to the protein fragments. Such conformational sampling is computationally intractable at this time. Within this context, we further examined the relative flexibility of the CaM domains using the technique of normal-mode Analysis (NMA). This technique was used to compute the vibrational properties of multiple energy minima generated from conformations explored in the molecular dynamics simulations. Conformations were selected to ensure that the conformational space explored

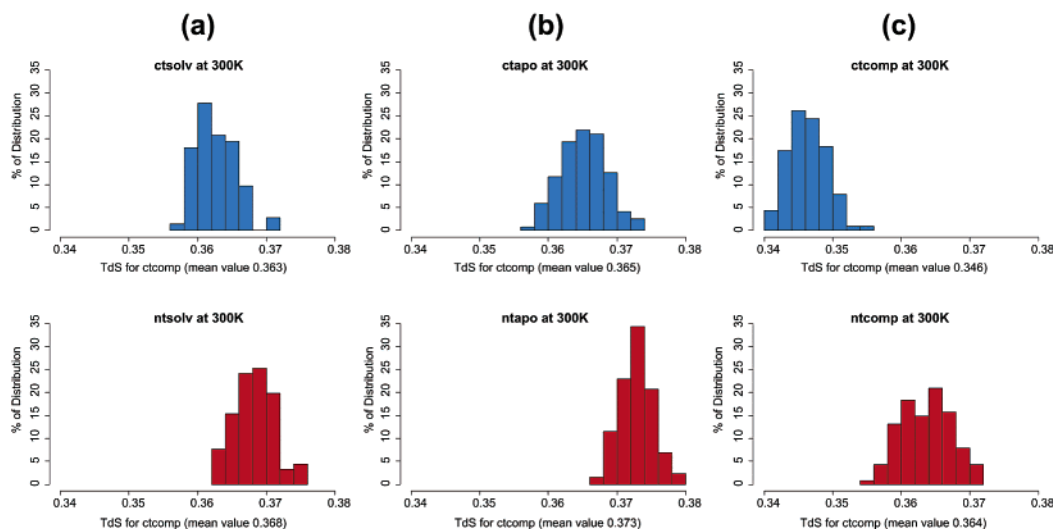


Figure 4. Histograms of the entropic contributions to the vibrational free energy at 300 K per degree of freedom for conformations generated from (a) Ca^{2+} -bound CaM, (b) Ca^{2+} -free CaM, and (c) the CaM target complex. Values for simulations of the C-term domain are shown at the top (in blue), and values for the N term are at the bottom (in red).

TABLE 2: Summary of Mean Configurational Entropic Contributions (in kcal/mol) to the Vibrational Free Energy at 300 K^a

simulation	N-domain entropy	C-domain entropy
Ca^{2+} -bound	0.368 (0.00290)	0.363 (0.00277)
Ca^{2+} expulsion	0.373 (0.00236)	0.365 (0.00320)
Ca^{2+} -CaM target complex	0.364 (0.00356)	0.346 (0.00270)

^a Values are presented per degree of freedom; standard deviations are presented in parentheses.

by the simulations has been fully characterized. The sampling here is sufficiently extensive (ca. 100 different conformations per trajectory) to ameliorate the problem of sensitivity to initial conditions for NMA studies of proteins.³¹

The distributions of (classical harmonic) configurational entropies calculated from the ca. 100 different conformations selected from each of the 5 different MD trajectories are shown in Figure 3. The total mean entropic contributions to the vibrational free energy at 300 K were 245.9 (ntsolv), 247.9 (ntapo), 234.5 (ntcomp), 220.5 (ctsolv), 221.2 (ctapo), and 209. (ctcomp) (values in kcal mol⁻¹ per degree of freedom to account for different system sizes).

In each experiment, the mean value of the distribution of configurational entropy values is larger for the N term than it is for the C term (Table 2); the statistical significance of these differences was established using the standard *t*-test. This provides clear evidence for the different character of the two Ca^{2+} -binding domains of CaM. Of particular interest is the observation that the difference is most evident in the simulations of the CaM target complex (Figure 4). Both the RMSD time series (Figure 2) and the configurational entropy values calculated in these experiments confirm that the N domain is more inherently flexible than the C domain of the protein. An examination of the density of states in the six systems³¹ shows that whereas the overall distribution is very similar (Figure 5 inset) the differences between the systems are largely confined to the low-frequency motions ($\leq 60 \text{ cm}^{-1}$) (Figure 5). Indeed, the decrease in entropy for a 1-cm⁻¹ increase in frequency is rapid and goes from -12% at 1 cm⁻¹ to -1% at 35 cm⁻¹. This also suggests that the major differences in flexibility result from collective displacements delocalized over the whole of each lobe rather than any specific region.

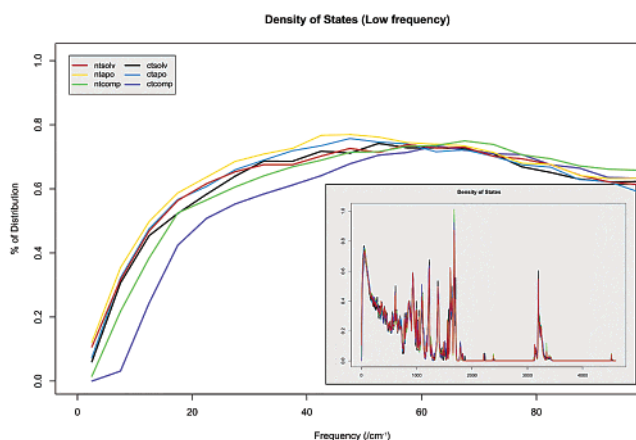


Figure 5. Density of states for the lowest-energy frequencies of vibration (main plot) and the full vibrational spectrum (inset) generated for the different trajectories. These are generated from the distribution of vibrational frequencies resulting from the normal-mode analyses performed on multiple conformations taken from the different MD trajectories.

These differences in flexibility of the N and C domains of CaM can be considered in the context of different properties of the two domains. The more-conserved C domain of the protein has a higher affinity for Ca^{2+} and a higher affinity for the majority of CaM targets.⁶

In this work, we see a distinct difference in the inherent flexibility of the N and C domains of CaM. Additionally, we see how the presence of a target peptide results in a more conserved and less flexible conformation for the C domain of the protein whereas the N domain retains much of the flexibility observed in the absence of the target peptide.

The identification of different functional roles for the domains,¹⁴ combined with the observation of a variety of different target binding modes⁷ (with the domains in a variety of relative spatial arrangements) helps to explain the diversity in the primary sequence observed for the plethora of CaM target sequences and suggests that target recognition is performed on a per-domain basis with separate motifs for the N and C domains of the protein.³² The noncontiguous nature of some targets has been further exposed in recent crystal structures.^{33,34} The identification of different functional roles of the two CaM

domains, coupled with their relative inherent flexibility and potential for global reorientation afforded by the central tether, is an essential element for CaM function. These observations provide considerable insight into the central high-affinity, low-specificity paradigm of CaM target interactions.

References and Notes

- (1) Vogel, H. J. *Biochem. Cell Biol.* **1994**, 72, 357–76.
- (2) Yap, K. L.; Kim, J.; Truong, K.; Sherman, M.; Yuan, T.; Ikura, M. *J. Struct. Funct. Genomics* **2001**, 1, 8–14.
- (3) Babu, Y. S.; Bugg, C. E.; Cook, W. J. *J. Mol. Biol.* **1988**, 204, 191–204.
- (4) Meador, W. E.; Means, A. R.; Quijcho, F. A. *Science (Washington, D.C.)* **1992**, 257, 1251–1254.
- (5) Ikura, M.; Clore, G. M.; Gronenborn, A. M.; Zhu, G.; Klee, C. B.; Bax, A. *Science (Washington, D.C.)* **1992**, 256, 632–638.
- (6) Bayley, P. M.; Findlay, W. A.; Martin, S. R. *Protein Sci.* **1996**, 5, 1215–1228.
- (7) Zhang, M.; Yuan, T. *Biochem. Cell Biol.* **1998**, 76, 313–23.
- (8) Dunker, K. A.; Brown, C. J.; Lawson, J. D.; Iakoucheva, L. M.; Obradovic, Z. *Biochemistry* **2002**, 41, 6573–6582.
- (9) Wilson, M. A.; Brunger, A. T. *J. Mol. Biol.* **2000**, 301, 1237.
- (10) Chou, J. J.; Li, S.; Klee, C. B.; Bax, A. *Nat. Struct. Biol.* **2001**, 8, 990–997.
- (11) Wriggers, W.; Mehler, E.; Pitici, F.; Weinstein, H.; Schulten, K. *Biophys. J.* **1998**, 74, 1622–1639.
- (12) Vigil, D.; Gallagher, S. C.; Trewella, J.; Garcia, A. E. *Biophys. J.* **2001**, 80, 2082–2092.
- (13) Barton, N. P. *Conformational Flexibility of Calmodulin*; Caves, L. S. D., Ed.; University of York: York, U.K., 2002 (in preparation).
- (14) Barth, A.; Martin, S. R.; Bayley, P. M. *J. Biol. Chem.* **1998**, 273, 2174–2183.
- (15) Wall, M. E.; Clarage, J. B.; Phillips, G. N. *Structure* **1997**, 5, 1599–1612.
- (16) Brooks, B. R.; Brucoleri, R. B.; Olafson, B. D.; States, D. J.; Swaminathan, S.; Karplus, M. *J. Comput. Chem.* **1983**, 4, 187–217.
- (17) MacKerell, A. D.; Bashford, D.; Bellott, M.; Dunbrack, R. L.; Evanseck, J. D.; Field, M. J.; Fischer, S.; Gao, J.; Guo, H.; Ha, S. *J. Phys. Chem. B* **1998**, 102, 3586–3616.
- (18) Jorgensen, W. L.; Chandrasekhar, J.; Madura, J. D.; Impey, R. W.; Klein, M. L. *J. Chem. Phys.* **1983**, 79, 926–935.
- (19) Brunger, A. T.; Karplus, M. *Proteins* **1988**, 4, 148–156.
- (20) Grubmueller, H. *Solvate 1.0*, version 1.0; 1996.
- (21) Marchand, S.; Roux, B. *Proteins* **1998**, 33, 265–284.
- (22) Berendsen, H.; Postma, J.; Van Gunsteren, W.; Dinola, A.; Haak, J. *J. Chem. Phys.* **1984**, 81, 3684–3690.
- (23) Kabsch, W. *Acta Crystallogr., Sect. A* **1976**, 32, 922–923.
- (24) Elber, R.; Karplus, M. *Science (Washington, D.C.)* **1987**, 235, 318–321.
- (25) Gentleman, R.; Ihaka, R. *R Statistical Language*, version 1.1.1.; Auckland, New Zealand, 2000.
- (26) Brooks, B. R.; Janezic, D.; Karplus, M. *J. Comput. Chem.* **1995**, 16, 1522–1542.
- (27) Fischer, S.; Smith, J. C.; Verma, C. S. *J. Phys. Chem. B* **2001**, 105, 8050–8055.
- (28) Amadei, A.; Linssen, A. B. M.; Berendsen, H. J. C. *Proteins* **1993**, 17, 412.
- (29) Caves, L. S.; Evanseck, J. D.; Karplus, M. *Protein Sci.* **1998**, 7, 649–666.
- (30) Zhang, M.; Tanaka, T.; Ikura, M. *Nat. Struct. Biol.* **1995**, 2, 758–767.
- (31) van Vlijmen, H. W. T.; Karplus, M. *J. Phys. Chem. B* **1999**, 103, 3009–3021.
- (32) Afshar, M.; Caves, L. S. D.; Hubbard, R. E.; Grassy, G.; Calas, B. A Unified Structural Model of Target Recognition in Calmodulin and Myosin Light Chains. Unpublished work, 1997.
- (33) Schumacher, M. A.; Rivard, A. F.; Bachinger, H. P.; Adelman, J. P. *Nature (London)* **2001**, 410, 1120–1124.
- (34) Drum, C. L.; Yan, S. Z.; Bard, J.; Shen, Y. Q.; Lu, D.; Soelaiman, S.; Grabarek, Z.; Bohm, A.; Tang, W. J. *Nature (London)* **2002**, 415, 396–402.